Polymer Chemistry

ROYAL SOCIETY OF CHEMISTRY

PAPER

View Article Online
View Journal | View Issue

Cite this: *Polym. Chem.*, 2023, **14**, 862

A fully bio-based Schiff base vitrimer with self-healing ability at room temperature†

Lin Jiang,‡ Yazhou Tian,‡ Xiaomu Wang, Junying Zhang, Jue Cheng * and Feng Gao *

The design of a green and renewable bio-based self-healing vitrimer has attracted extensive attention due to the increasing emphasis on an environment friendly society. However, it remains a challenge to design and fabricate a fully bio-based vitrimer with a room temperature self-healing ability without sacrificing the aqueous stability and mechanical performance. In this work, a dialdehyde monomer was designed and synthesized using vanillin, 2,5-furandicarboxylic acid, and succinic acid. A fully bio-based Schiff base vitrimer was prepared with the bio-based curing agent Priamine 1071 (FDV-1071 and SCV-1071). The synthetic process was simple under mild conditions at room temperature without any catalyst. The rigid polyphenyl and furan structure of the dialdehyde monomer endowed the vitrimer with reinforced mechanical performance, and the tensile strength and T_g of FDV-1071 reached 2.45 MPa and 25.14 °C, respectively. The fully bio-based vitrimer containing both an imine bond and an active ester bond showed excellent thermal reversibility and self-healing properties. FDV-1071 slices allowed multiple reprocessing cycles at 120 °C and 10 MPa and still retained the self-healing ability even at room temperature. In addition, the aliphatic chains of Priamine 1071 increased the hydrophobicity of the vitrimer, greatly enhancing the stability in the aqueous environment, and the degradability of the vitrimer was tunable by the introduction of an organic solvent.

Received 11th July 2022,
Accepted 1st January 2023

DOI: 10.1039/d2py00900e

rsc.li/polymers

1. Introduction

A Schiff-base vitrimer,[1–6] one of the most significant vitrimers, has drawn increasing attention due to the convenient and catalyst-free reaction process and has been applied in coating, composite materials, biomedical materials, *etc.*[7–9] A Schiff-base vitrimer is usually designed and prepared using polyamines and polyaldehydes.[10–12] Compared with polyamines, polyaldehydes have higher designability and selectivity. However, most polyaldehydes come from petroleum-based materials, which not only affect environmental protection but also inhibit sustainable development.[13–16]

Recently, the synthesis of bio-based polyaldehydes has aroused researchers' wide interest. Wei *et al.*[17] used natural polysaccharides to oxidize and prepare bio-based polyaldehydes and then crosslinked them with *N*-carboxyethyl chitosan (CEC) to obtain a biocompatible polysaccharide-based self-healing hydrogel, which could achieve a repair efficiency of 95%. Dong *et al.*[5] crosslinked amine chitosan with a long-chain dialdehyde (PEG-DA) to prepare a bio-based Schiff alkaline hydrogel, which has excellent electrical conductivity and self-healing ability.

In order to improve the biomass content, vanillin,[18–20] a bio-based monomer derived from lignin, has been used to synthesize bio-based polyaldehydes. Zhang *et al.*[21] synthesized a vanillin-based aldehyde compound with a biomass content of 58.9%. After being cured with 4-AFD and tris (2-aminoethyl) amine, the vitrimer showed excellent self-healing properties with the addition of a catalytic amount of amine. Geng *et al.*[11] synthesized a dialdehyde monomer (DAV) from vanillin and 1,4-dibromo butane with a biomass content of 84.3%. After being respectively cured with different proportions of a mixed curing agent of diethylenetriamine and tris (2-aminoethyl) amine, three polyschiff vitrimers were prepared and sample 1 was self-healed after 1 hour at 180 °C. Wang *et al.*[22] synthesized a trifunctional aldehyde compound (TFMP) from vanillin and phosphorus oxychloride with a biomass content of 90.6% and then cross-linked it with three binary amine curing agents to obtain three Schiff base covalent adaptable networks (CANs). The Schiff base CANs films could be recovered into complete films in 10 min at 180 °C under 15 MPa pressure. Although many biomass aldehydes have been syn-

Key Laboratory of Carbon Fiber and Functional Polymers, Ministry of Education, Beijing University of Chemical Technology, Beijing 100029, People's Republic of China. E-mail: chengjue@mail.buct.edu.cn, gaofeng@mail.buct.edu.cn; Tel: +86 64425439

†Electronic supplementary information (ESI) available. See DOI: https://doi.org/10.1039/d2py00900e

‡These authors contributed equally to this work.

thesized, they all have less bio-mass content, and amines are non-biobased, which greatly reduces the biomass content. Therefore, the biomass content of Schiff base vitrimers needs to be further improved.[23] In addition, the temperature requirements for self-healing and reprocessing performance in the above research studies are high,[24–26] so Schiff base vitrimers that can self-heal at room temperature need to be further studied because vitrimers that can self-heal at room temperature will be more widely used.

2,5-Furandicarboxylic acid and succinic acid are bio-based platform compounds with high added value announced by the Department of Energy in 2004.[27–29] These two compounds have been used in the synthesis of epoxy resins, polyurethanes, and benzoxazine resins.[30,31] However, the synthesis of Schiff base aldehydes has not been reported yet.

In this work, we designed a fully bio-based dialdehyde monomer derived from 2,5-furandicarboxylic acid, succinic acid and vanillin, followed by curing with the bio-based curing agent Priamine 1071[32] to obtain a fully bio-based Schiff base vitrimer without a catalyst. The hydrophobic matrix was expected to protect the Schiff-base connection from hydrolysis, and the mechanical performance could be tuned by adjusting the rigid and soft segments in the vitrimer. The results were consistent with our hypothesis, and the tensile strength reached up to 2.5 MPa which was significantly higher than that of the vitrimer built from Priamine 1071 and furan aldehyde (0.7 MPa). At the same time, vitrimers prepared in this work showed the self-healing ability due to the abundant imine bonds. A scratch on the surface of the vitrimer disappeared after 120 min at room temperature. The reversibility of the imine rapidly increased when the temperature was increased, and the time taken for the disappearance of the surface scratch reduced to 15 min when the temperature was increased to 120 °C. A great recycling ability was also presented by the vitrimer, and the fragments were able to reassemble back at 120 °C under 10 MPa pressure retaining more than 90% mechanical strength. In addition, degradation of the vitrimer was achieved in a mixture of organic solvents and acid or alkaline aqueous solutions.

2. Materials and methods

2.1 Materials

Vanillin was provided by San Chemical Technology Co., Ltd. 2,5-Furandicarboxylic acid and succinyl chloride were prepared in our laboratory before.[33] Sodium hydroxide (NaOH), ethyl acetate (EAC), ethanol (EtOH) and tetrahydrofuran (THF) were provided by Beijing Chemical Works. Priamine 1071 was provided by CRODA.

2.2 Synthesis of a fully bio-based dialdehyde monomer

In our previous work,[34] we have introduced the steps for the synthesis of dialdehyde monomers. Vanillin (0.4 mol) was added to NaOH (0.41 mol) aqueous solution (200 mL) and stirred for 10 min to obtain vanillin sodium salt solution. 2,5-Furandicarbonyl dichloride (0.2 mol) was dissolved in EAC (200 mL) and transferred to a drop funnel after full dissolution, and then it was added dropwise into a sodium salt solution under the conditions of 0 °C ice bath and magnetic agitation. Then it was reacted at 0 °C for 2 h and 50 °C for 5 h. After the reaction, the upper solution was washed with sodium hydroxide aqueous solution three times and then washed with water three times. A fully bio-based dialdehyde monomer (FDV) was prepared after vacuum drying at 60 °C for 24 h. The preparation method for SCV was the same as that for FDV. The reaction diagram of the fully bio-based dialdehyde monomer is shown in Fig. 1(a).

2.3 Preparation of fully bio-based polyimine vitrimers

8.5 g of FDV (0.02 mol) was completely dissolved in 30 mL of EAC, and 10.82 g of Priamine 1071 (0.018 mol) was added to the monomer solution drop by drop slowly, and immediately stirred vigorously for 10 min. The mixture was charged into a round bowl of aluminum foil to remove the solvent at room temperature over 5 h. The precured vitrimer was obtained by curing at 60 °C for 3 h in a vacuum dryer. The original sample of FDV-1071 was cured for 3 h in an oven at 120 °C. The preparation method for SCV-1071 was the same as that for FDV-1071. The synthesis route to fully bio-based polyimine vitrimers is displayed in Fig. 1(b).

2.4 Characterization

Fourier transform infrared (FTIR) spectroscopy. The FTIR spectra were recorded on a Nicolet Nexus 670 spectrometer in the wavelength range of 400–4000 cm^{-1} at a resolution of 4 cm^{-1}. The KBr tablet method was used to characterize the synthesis of the fully bio-based dialdehyde monomer and trace the curing of the fully bio-based Schiff base vitrimer.

Nuclear magnetic resonance (NMR). A Bruker Avance III HD (400 MHz) was used to determine the ^1H NMR spectra to characterize the synthesis of the fully bio-based monomer. $CDCl_3$ was used as the solvent for ^1H NMR detection. TMS was used as the internal standard.

Differential scanning calorimetry (DSC). The vitrification transition temperature of the fully bio-based Schiff base vitrimer was analyzed by DSC in a nitrogen atmosphere using a TA Instruments Q20. Temperature program: heat from 25 °C to 120 °C. The temperature then immediately drops to −60 °C and gradually rises to 60 °C at 10 °C min^{-1}. The glass transition temperature measured by DSC was recorded as T_{ga}.

Thermogravimetric analysis (TGA). TGA was performed using the TA Instruments Q500 to evaluate the thermal stability of a fully bio-based Schiff base vitrimer over a temperature range of 25–800 °C at a heating rate of 10 °C min^{-1} in a nitrogen atmosphere.

Dynamic mechanical analyses (DMA). Dynamic mechanical analysis was performed using TA Instruments Q800. The energy storage modulus and tan δ curves of the vitrimer were measured in the range of −80 to −100 °C (3 °C min^{-1}). The peak of the tan δ curve revealed the vitrification transition temperature of the fully bio-based Schiff base vitrimer. The

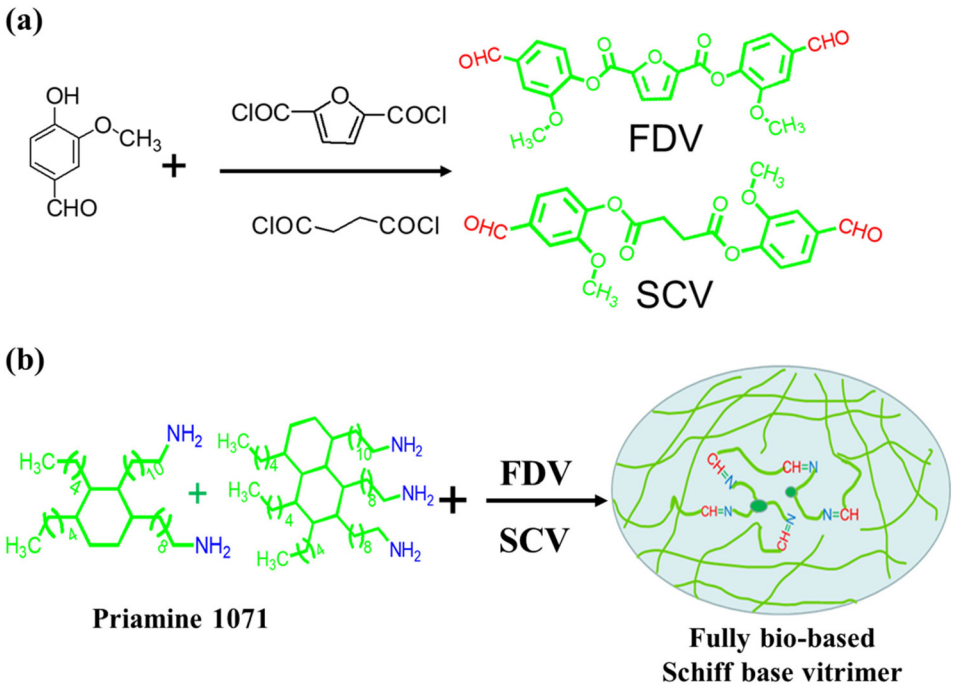

Fig. 1 Synthetic route to (a) fully bio-based dialdehyde monomer FDV and SCV and (b) fully bio-based Schiff base vitrimer.

vitrification transition temperature measured by DMA was recorded as T_{gb}. The spline size is 25 mm × 4 mm × 0.25 mm.

Reprocessing experiment. The original vitrimer was cut into pieces and placed in a metal mold. The sample was pressed by a hot press (760p-24b) at 120 °C and 10 MPa. After natural cooling, the sample was taken out to obtain the 1st recycled sample. Similarly, the 2nd recycled sample was obtained by shearing and pressing the 1st recycled sample. The 3rd recycled sample was obtained by shearing and pressing the 2nd recycled sample.

Tensile testing. The tensile strength of the material was tested on a universal testing machine (SANS UTM5205XHD). Dumbbell shaped splines were made by pressing for testing. In order to obtain stable repeatability of data, this paper tested 5 splines for each group of samples and the mean value was calculated.

Stress relaxation. A dynamic mechanical analyzer (TA Instruments Q800) was used to test the stress relaxation of the vitrimer material with 5% constant strain and 1×10^{-3} N force. The spline size is 25 mm × 4 mm × 0.25 mm. The decrease in the stress relaxation modulus and the corresponding time were recorded.

Self-healing experiment. The polyimine vitrimer of FDV-1071 was placed at room temperature of 120 °C, 60 °C and 25 °C, respectively, for the self-healing test. The healing of the scratch was observed under an optical microscope.

Water contact angle test. The water contact angle (CA) of the vitrimer material was measured using the water contact angle tester DSA10-MK2.

Degradation test. FDV-1071 was placed in hydrochloric acid aqueous solution (1 M HCl, 0.1 M HCl) and NaOH aqueous solution (1 M NaOH, 0.1 M NaOH) with different concentrations at 25 °C for 96 h to observe the degradation. Then, the whole bio-based Schiff base vitrimer material was placed in the acid–base mixed solution (l M HCl + EA, l M HCl + THF, l M NaOH + EA and 1 M NaOH + THF with v : v, 8 : 2, respectively) at 25 °C for 8 hours to record the degradation process.

3. Results and discussion

3.1 Synthesis and characterization of FDV and SCV

Vanillin was linked by 2,5-furandiformyl chloride and succinyl chloride through a one-step reaction with ethyl acetate as the solvent constructing the dialdehyde monomers for the vitrimer which was abbreviated as FDV and SCV, respectively. The structure of FDV and SCV was examined by FTIR and ^{1}H NMR, and the corresponding spectrum is given in Fig. 2. The characteristic peak of C=O located at 1745 cm^{-1} shown in Fig. 2(a) indicates the formation of the ester groups between the phenolic hydroxyl groups and the acyl chloride. At the same time, the peak located at 1700 cm^{-1} indicated that the aldehyde groups on the vanillin were preserved during the reaction. The chemical structures of FDV and SCV were further confirmed by ^{1}H NMR spectra which are demonstrated in Fig. 2(b) and (c). A chemical shift of the proton from –CHO groups on the vanillin was around 10.08 ppm, and that of –CH_3 was around 3.92 ppm. The chemical shift in the range of 7.21–7.65 ppm was the characteristic spectrum of the aromatic ring in vanillin. The peaks at around 7.86 in Fig. 2(b) indicated the existence of the furan structure in FDV. The peak at around 3.12 ppm in Fig. 2(c) was assigned to the hydrogen of the methylene from succinyl chloride. Thus, both the FTIR and ^{1}H

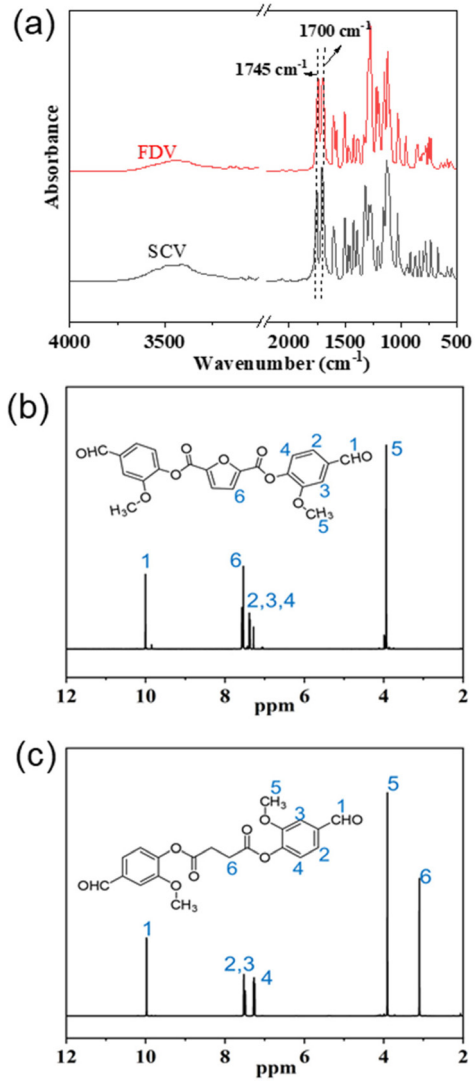

Fig. 2 FTIR spectra (a) and ^{1}H NMR spectra of FDV (b) and SCV (c).

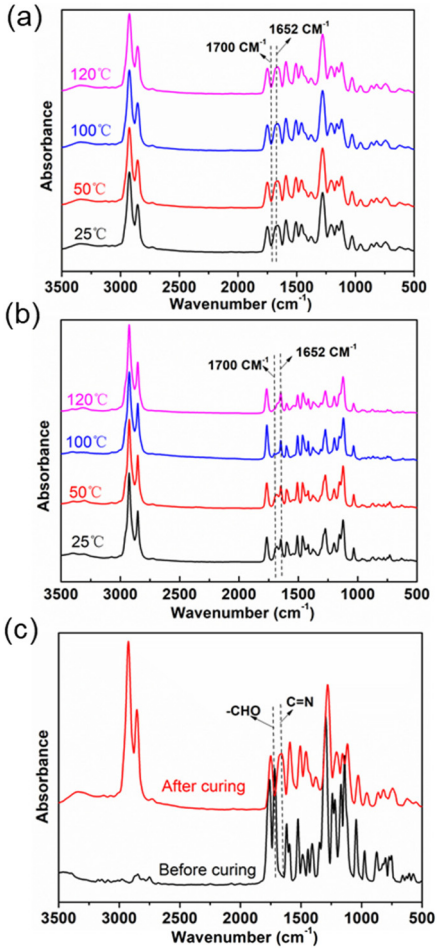

Fig. 3 The tracing of the Schiff-base reaction by FTIR; (a) the spectra of FDV-1071 and (b) SCV-1071. (c) FTIR spectra of FDV-1071 before and after curing.

NMR characterization methods indicated the successful synthesis of FDV and SCV. The structures of FDV, SCV and the raw materials used in this work were also examined by ^{1}H NMR, ^{13}C NMR and HRMS spectra, which are presented in the ESI section.†

3.2 Preparation and structural characterization of the fully bio-based Schiff base vitrimer

The change in the network structure after vitrimer curing at different curing temperatures was examined by FTIR which is shown in Fig. 3. The FTIR spectra of FDV-1071 and SCV-1071 are shown in Fig. 3(a) and (b), respectively. As demonstrated in Fig. 3(a), the peaks located at around 1700 cm^{-1} and 1652 cm^{-1} belonged to the vibration of –CHO and –C═N, respectively. Almost no –CHO was detected in the FDV-1071 system with the curing temperature ranging from 25 to 120 °C. However, the curing velocity was significantly lower for the SCV-1071 system. The characteristic peak for –CHO totally disappeared when the curing temperature reached 120 °C. The difference in the curing speed between these 2 systems was attributed to the higher reactivity of 2,5-furandiformyl chloride than that of succinyl chloride which is due to the conjugation effect of furan. Fig. 3(c) shows the FTIR spectra of FDV after curing with Priamine 1071 as the crosslinker. The peak of –CHO at 1700 cm^{-1} completely disappeared with the appearance of the peak located at 1652 cm^{-1} indicating the formation of C═N connections in the matrix. The peak of the ester group C═O at 1745 cm^{-1} always exists. The results presented in Fig. 3 showed the complete reaction between the dialdehyde monomer and Priamine 1071 in ethyl acetate consisting with the ^{1}H NMR characterization. Moreover, the reaction of the SCV-1071 system was able to take place even at room temperature.

3.3 The reprocessability of the vitrimer

The polyimine vitrimer has reprocessability due to the presence of reversible dynamic bonds which is intuitively demonstrated in Fig. 4. As shown in Fig. 4(a), after shearing, a

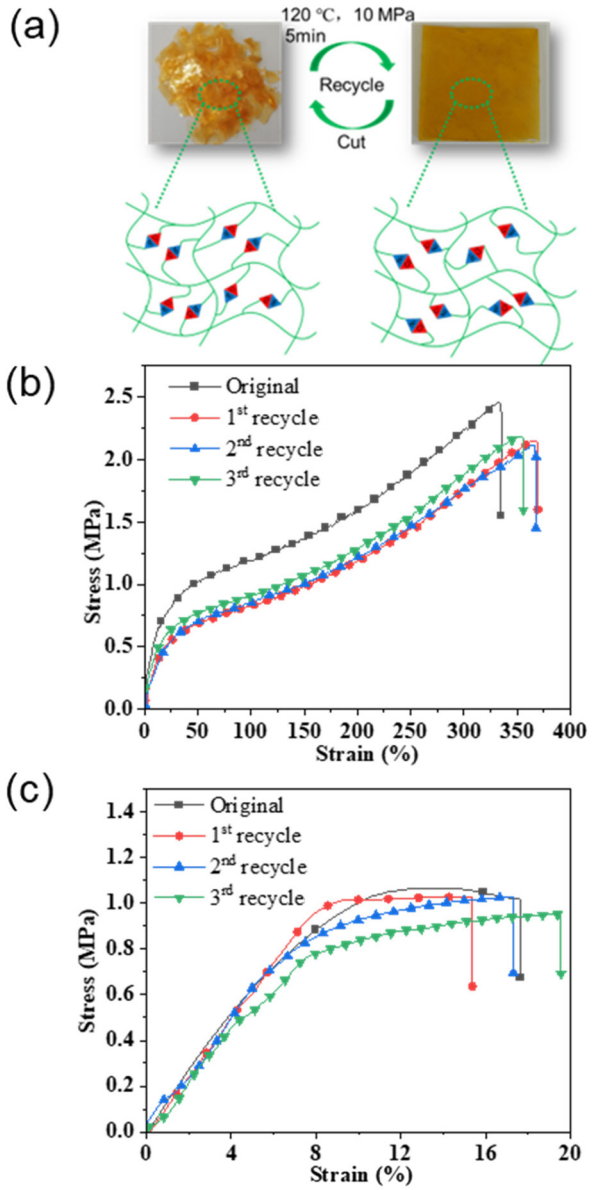

Fig. 4 Schematic representation of reprocessing of vitrimer (a); tensile test of FDV-1071 (b) and SCV-1071 (c).

polymer can be hot-pressed at 120 °C and 10 MPa for 5 min to successfully obtain a polymer film. The principle of this reprocessing is the exchange reaction of dynamic imine bonds within the polymer crosslinking network. We reprocessed the fully bio-based polyimine vitrimer 3 times according to the reprocessing experiment and conducted tensile tests on the polymer films obtained after each cycle. As shown in Fig. 4(b) and (c), the tensile strength of FDV-1071 was 2.45 ± 0.08 MPa and changed to 2.21 ± 0.08, 2.16 ± 0.09 and 2.32 ± 0.11 MPa after the 1st, 2nd and 3rd reprocessing cycles, respectively. A similar trend was also reflected by the sample sets of SCV-1071. As demonstrated in Fig. 1, a 3D network structure was generated by the vitrimer designed in this work which should hardly show the reprocessing ability. However, more than 90% of the tensile strength was recovered by FDV-1071 and SCV-1071, presenting the integrity and the homogeneity of the matrix after reprocessing. The tensile strength values of the three reprocessing cycles showed no significant difference, indicating that the dynamic bond exchange by the imine connection did not change the crosslinking density of the vitrimer. The elongation at break of the vitrimer showed a similar trend. The value for FDV-1071 was 340 ± 14.2% initially which turned to be 365 ± 21.5%, 359 ± 12.7% and 348 ± 14.6% after the 1st, 2nd and 3rd reprocessing cycle correspondingly showing no significant difference. The elongation at break of SCV-1071 was consistent with that of FDV-1071 which was due to the dynamic exchange mechanism of the imine bonds in the vitrimer. The maximum tensile strength of FDV-1071 was around 2.45 ± 0.08 MPa significantly higher than that of SCV-1071 which was 1.04 ± 0.02 MPa. This difference was mainly attributed to the high rigidity of the furan structure in FDV-1071. The tensile test results of the membranes before and after reprocessing are recorded in Table 1. The low aromatic content and the long aliphatic chain length in the crosslinking network weakened the tensile strength.[36] However, the elongation at break was greatly enhanced, and the high toughness and the elastic nature broadened the application area of the vitrimer synthesized in the present work.

3.4 The thermal properties of the vitrimer

The glass transition, thermal stability and thermal-mechanical properties of the vitrimer membranes were characterized by DSC, TGA, and DMA, respectively, and the corresponding results are presented in Table 2 and Fig. 5. The curves plotted in Fig. 5(a) represent the glass transition temperature characterized by DSC (T_{ga}), and the value for FDV-1071 and SCV-1071 was 7.25 and −4.96 °C, respectively. The TGA curves reflected the thermal stability of the vitrimers. As shown in Fig. 5(b), FDV-1071 and SCV-1071 have similar carbon residues which were only around 10%. This reflects the fact that abundant flexible long aliphatic chains are present in the network of the vitrimer. Fig. 5(c) presents the DMA analysis results, indicating that the storage modulus (E') of FDV-1071 was higher than that of SCV-1071. The glass transition temperature characterized by DMA was abbreviated as T_{gb}, which was reflected by the position of the tan δ peaks in Fig. 5(d). The T_{gb} of FDV-1071 and SCV-1071 was 25.14 and 8.32 °C, respectively,

Table 1 Mechanical properties of FDV-1071 and SCV-1071

Samples	Status	Tensile strength at break (MPa)	Elongation at break (%)
FDV-1071	Original	2.45 ± 0.08s	340 ± 14.2
	1st recycle	2.21 ± 0.08	365 ± 21.5
	2nd recycle	2.16 ± 0.09	359 ± 12.7
	3rd recycle	2.32 ± 0.11	348 ± 14.6
SCV-1071	Original	1.04 ± 0.02	17.9 ± 0.81
	1st recycle	1.02 ± 0.02	16.1 ± 1.42
	2nd recycle	1.03 ± 0.02	16.9 ± 1.08
	3rd recycle	0.95 ± 0.01	19.2 ± 1.08

Table 2 The thermal properties, thermal stability and v_e of FDV-1071 and SCV-1071

Material	T_{ga} (°C)	T_{gb} (°C)	Char yield (%)	v_e [a] (mol m^{-3})
FDV-1071	7.3 ± 0.18 °C	25.1 ± 0.36 °C	10.12	218 ± 13
SCV-1071	−5.0 ± 0.11 °C	8.3 ± 0.22 °C	9.98	120 ± 9

T_{ga} was obtained from the DSC measurement; T_{gb} was obtained from the DMA test [a] The crosslinking density was calculated based on the formula: $v_e = E_r/6RT$ with the plateau model and the temperature was set as T_g + 40 °C.

which was consistent with the DSC results. These results indicated that FDV-1071 presented higher thermal stability and better thermo-mechanical properties than SCV-1071, and the speculation was made that the crosslinking density of FDV-1071 was higher than that of SCV-1071. The crosslinking density (v_e) was estimated quantitatively based on the formula: $v_e = E_r/6RT$ with the plateau model and the temperature was set as T_g + 30 °C, T_g + 40 °C and T_g + 60 °C, respectively. The v_e values for FDV-1071 and SCV-1071 were 218 ± 13 and 120 ± 9 mol m^{-3}, respectively, when the testing temperature was set as T_g + 30 °C. The calculated results when the temperature was set as T_g + 40 °C and T_g + 60 °C followed the same trend which are presented in the ESI section.† As expected, the high crosslinking density of FDV-1071 lead to high mechanical and thermal properties. In addition, the rigid furan structures of FDV-1071 also reinforced the network structure, enhancing the thermal stability and the mechanical performances. The corresponding data of thermal properties, thermal stability and v_e of FDV-1071 and SCV-1071 are shown in Table 2.

3.5 Thermal stress relaxation

The stress relaxation experiments were carried out to study the flow behavior of polymer networks at different temperatures and can be used to evaluate the dynamic exchange ability of the vitrimer. The characteristic relaxation time (τ^*) is defined as the time required for the relaxation modulus G_0 to decrease to $1/e$ of its initial value. The relationship between τ^* and the temperature for FDV-1071 and SCV-1071 is demonstrated in

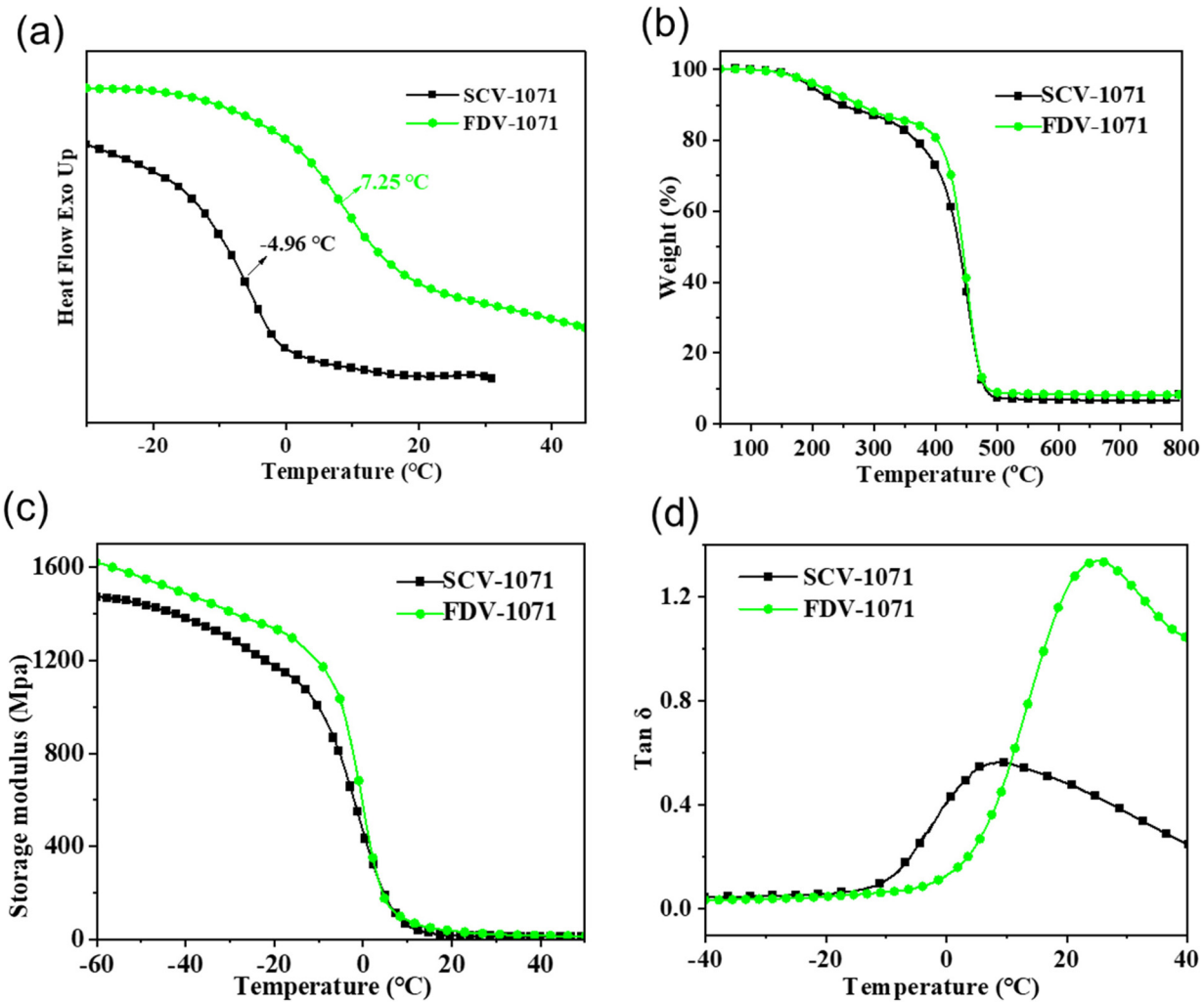

Fig. 5 DSC measurement (a), TGA (b), and DMA (c) and (d) of the 1st recycled vitrimers.

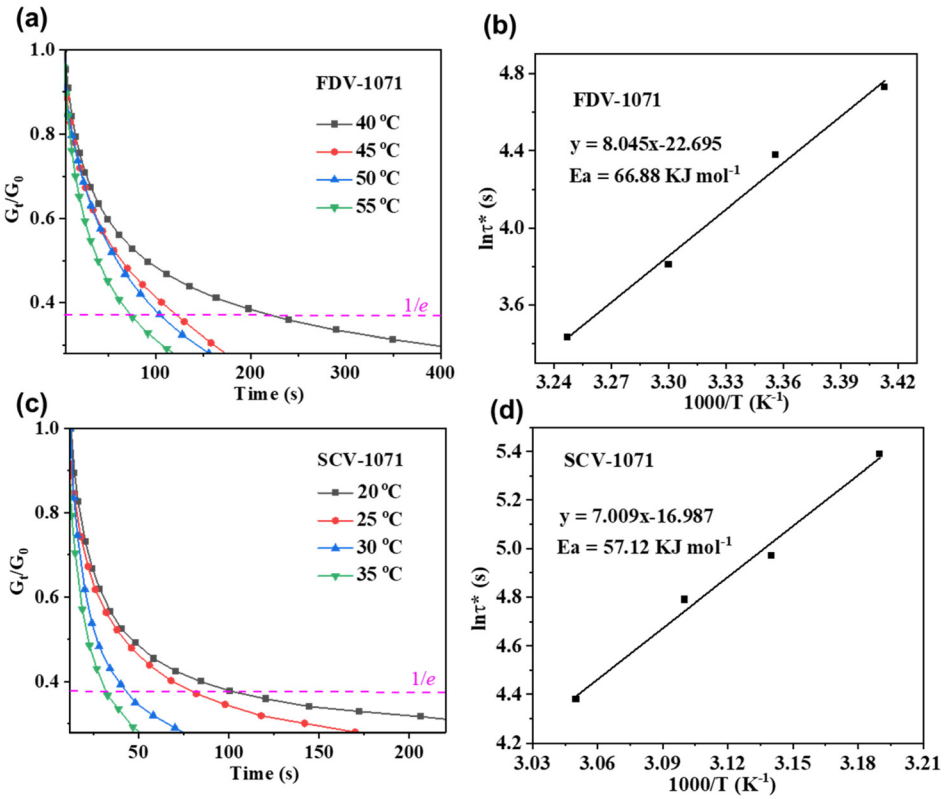

Fig. 6 Stress relaxation plots of (a) FDV-1071 and (c) SCV-1071 at different temperatures and fitting of the relaxation times to the Arrhenius equation for (b) FDV-1071 and (d) SCV-1071.

Fig. 6(a) and (c), respectively. The activation energy (E_a) of the chain exchange was calculated by the linear fitting between ln (τ^*) and 1000 K^{-1} according to the Arrhenius law: $\tau^*(T) = \tau_0 \exp(E_a/RT)$, which is presented in Fig. 6(b) and (d). According to the slope of the fitting curves, E_a of FDV-1071 and SCV-1071 was 66.88 and 57.12 kJ mol^{-1}, respectively. The calculated E_a falls into the reasonable E_a range (33.5–129 kJ mol^{-1}) for polyimines which is indicated by the previous publication.[35] FDV-1071 showed higher E_a than that of SCV-1071, presenting a lower thermal stress relaxation ability. The proposed reason was that the dense crosslinking network and the rigid furan structure of FDV-1071 limited the chain diffusion and restrained the bond exchange process. This result was also consistent with the thermal stress relaxation. Both FDV-1071 and SCV-1071 demonstrated a stress relaxation ability in the temperature ranging from 20 to 55 °C, indicating that these sample sets should have the self-healing ability under these conditions.

3.6 Evaluation of the self-healing ability

The reprocessability and stress relaxation of FDV-1071 and SCV-1071 were characterized in the previous section, which indicated that the sample sets should have the self-healing ability. Herein, the surface scratch recovery ability of these two sample sets at different temperatures was evaluated and compared, which is demonstrated in Fig. 7. The optical microscopy image presented in Fig. 7(a) shows that the scratch on the surface of FDV-1071 disappeared after 15 min at 120 °C without pressure, indicating the rapid self-healing strength at the reprocessing temperature. The time required to eliminate the scratch on FDV-1071 increased to 20 min when the temperature was raised to 60 °C as demonstrated in Fig. 7(b). However, it still showed excellent self-healing ability under this condition. As shown in Fig. 7(c), the FDV-1071 vitrimer still showed the self-healing ability even at room temperature, and the time required to eliminate the surface scratch at 25 °C was around 2 hours. The surface scratch recovery tests indicated that the dynamic imine bonds endowed the fully bio-based Schiff base vitrimer FDV-1071 with the self-healing ability even at room temperature which has the bright future in the industry.

3.7 Degradation of the vitrimer

Vitrimers based on the imine exchange reaction fabricated from vanillin showed the ability to decompose to amines and aldehydes in acidic organic solvents.[36] The degradation velocity of the fully bio-based vitrimer prepared in this work in different environments is measured and demonstrated in Fig. 8. No significant difference was observed when the sample slices were immersed in 1 M HCl, 0.1 M HCl, 1 M NaOH and 0.1 M NaOH solutions for 72 hours at room temperature, respectively. The mass change of the samples was recorded

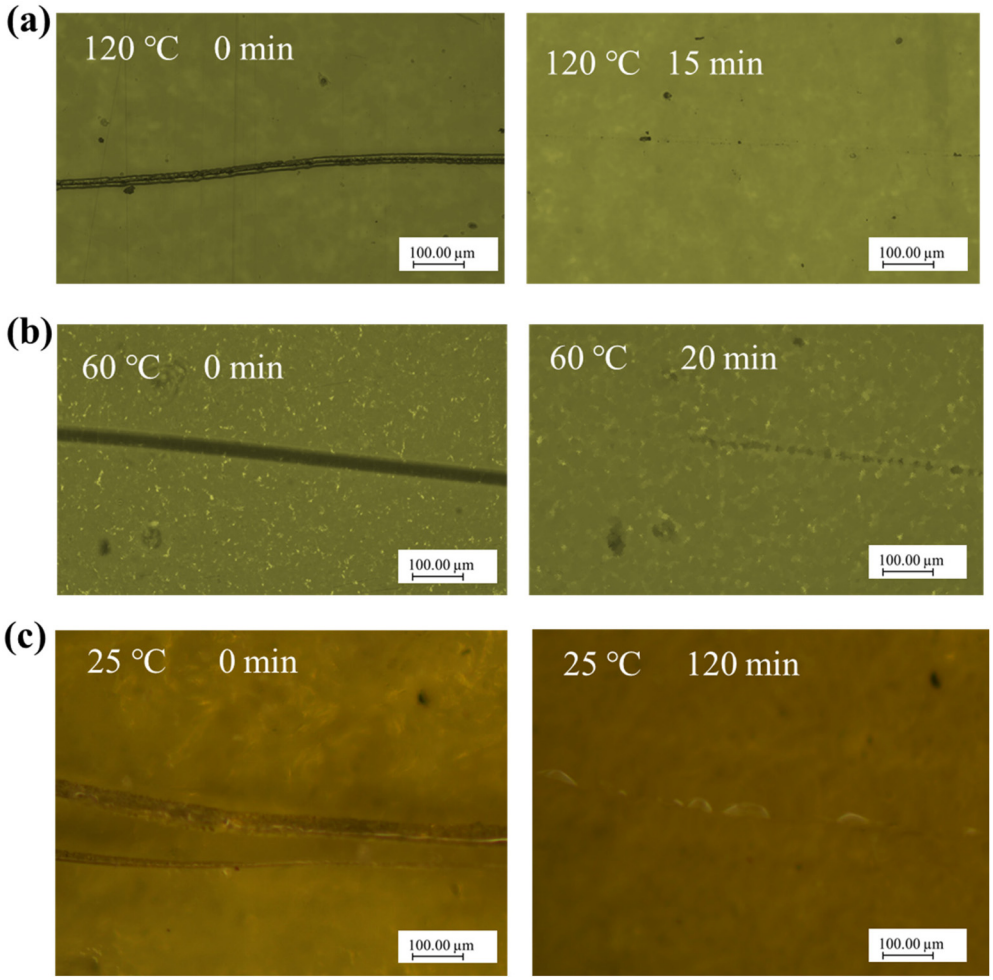

Fig. 7 Optical microscopy images of scratched FDV-1071 (a) at 120 °C, (b) at 60 °C, and (c) at 25 °C.

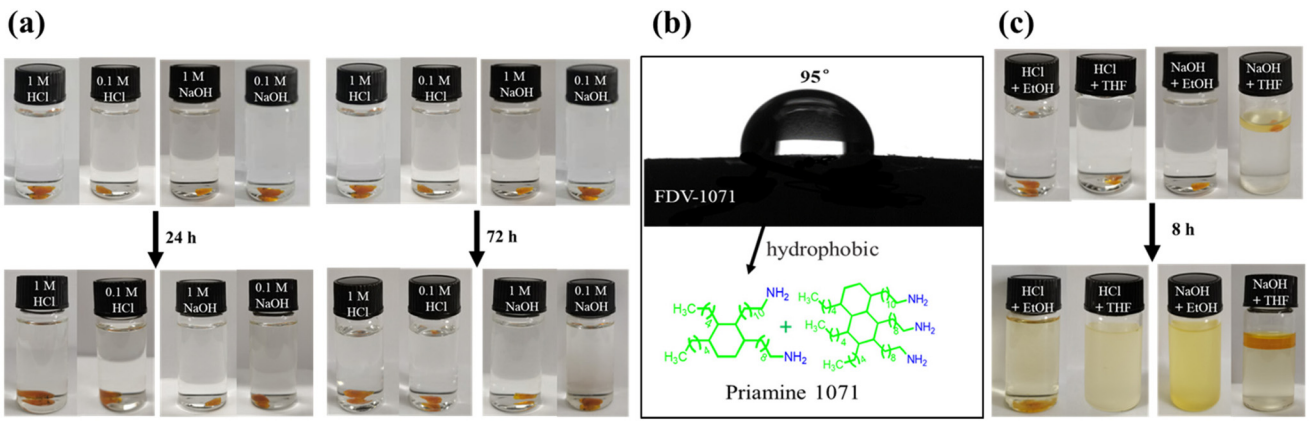

Fig. 8 (a) Digital photo of FDV-1071 in the aqueous solution of HCl and NaOH, (b) water contact angle of FDV-1071 and (c) digital photo of FDV-1071 in 1 M HCl + EtOH (THF) (v : v, 8 : 2) and in 1 M NaOH + EtOH (THF) (v : v, 8 : 2).

showing no significant change during this process which is presented in the ESI section.† The thermosets containing imine bonds should hydrolyze rapidly under the acidic conditions, and those containing ester connections should degrade in the alkaline environment. However, the fully bio-based vitrimer showed outstanding stability in the acidic/alkaline aqueous environment. The reason behind was that the aliphatic chains contained by Priamine 1071 increased the hydro-

phobicity of the vitrimer protecting the imine and ester bonds from water. The hydrophilicity was evaluated using the contact angles presented in Fig. 8(b). The water contact angle of FDV-1071 was around 95°, showing the hydrophobic nature. The influence of the organic solvent on the degradation velocity of the fully bio-based vitrimer is also explored and presented in Fig. 8(c). FDV-1071 slices were placed in l M HCl + EtOH, lM HCl + THF, l M NaOH + EtOH, and l M NaOH + THF mixed solutions (v : v, 8 : 2). After 8 hours, we found that FDV-1071 completely degraded and dissolved in l M HCl + THF, l M NaOH + EtOH, and l M NaOH + THF mixed solutions, and partially degraded in l M HCl + EtOH solution. This indicated that the introduction of organic solvents was able to enhance the wettability of the fully bio-based vitrimer accelerating the hydrolysis of the imine and ester bonds in the crosslinking network. The hydrophobic vitrimer FDV-1071 showed outstanding stability in the presence of water, making it promising to be used as the structural thermoset in the application. The degradation velocity was tunable by introducing the organic solvent, which makes it easy to remove on demand.

4. Conclusion

From the perspective of resources and environment, this work proposed a simple and efficient method to prepare two types of fully bio-based Schiff base vitrimers (FDV-1071 and SCV-1071). All the feedstocks (vanillin, 2,5-furandicarbonyl dichloride, succinyl chloride, and Priamine 1071) were bio-based and from the sustainable resources. The rigid polyphenyl and furan structures of the FDV-1071 reinforced the network structure of FDV-1071, and the tensile strength of the vitrimer was enhanced to 2.5 MPa even with the use of Priamine 1071 containing abundant flexible aliphatic chains. The FDV-1071 vitrimer contained abundant imine bonds and showed excellent reprocessability allowing multiple reprocessing cycles at 120 °C and 10 MPa retaining more than 90% mechanical strength. The vitrimer retained the rapid self-healing ability even at room temperature and showed the ability to heal the scratch on the surface within 120 min. The aliphatic chains of Priamine 1071 greatly improved the stability of the vitrimer in acidic and basic aqueous environments, and the degradation of the vitrimer was tunable by the introduction of the organic solvent. The design of the fully bio-based Schiff base vitrimer from the sustainable raw materials in this work contributes to the solution of the problems of resource shortage and environmental pollution by providing guidance for developing a novel and sustainable strategy for the design of fully bio-based materials.

Conflicts of interest

There are no conflicts to declare.

Acknowledgements

The work described in this article was supported by funding from Natural Science Foundation of China (22208012).

References

1 P. Taynton, H. Ni, C. Zhu, K. Yu, S. Loob, Y. Jin, H. J. Qi and W. Zhang, *Adv. Mater.*, 2016, **28**, 2904–2909.
2 Y. Xin and J. Yuan, *Polym. Chem.*, 2012, **3**, 3045–3055.
3 Y. Jin, Y. Zhu and W. Zhang, *CrystEngComm*, 2013, **15**, 1484–1499.
4 H. An, Y. Bo, D. Chen, Y. Wang, H. Wang, Y. He and J. Qin, *RSC Adv.*, 2020, **10**, 11300–11310.
5 R. Dong, X. Zhao, B. Guo and P. X. Ma, *ACS Appl. Mater. Interfaces*, 2016, **8**, 17138–17150.
6 P. Zhao, Z. Liu, X. Wang, Y. T. Pan, I. Kuehnert, M. Gehde, D. Y. Wang and A. Leuteritz, *RSC Adv.*, 2018, **8**, 42189–42199.
7 W. Denissen, J. M. Winne and F. E. Du Prez, *Chem. Sci.*, 2016, **7**, 30–38.
8 S. Dong, L. Yang, P. Zhang, H. Wang and J. Cui, *Polymer*, 2022, **239**, 124434.
9 G. Oliveux, L. O. Dandy and G. A. Leeke, *Prog. Mater. Sci.*, 2015, **72**, 61–99.
10 Y. Y. Liu, J. He, Y. D. Li, X. L. Zhao and J. B. Zeng, *Compos. Commun.*, 2020, **22**, 100445.
11 H. Geng, Y. Wang, Q. Yu, S. Gu, Y. Zhou, W. Xu, X. Zhang and D. Ye, *ACS Sustainable Chem. Eng.*, 2018, **6**, 15463–15470.
12 X. Xu, S. Ma, S. Wang, J. Wu, Q. Li, N. Lu, Y. Liu, J. Yang, J. Feng and J. Zhu, *J. Mater. Chem. A*, 2020, **8**, 11261–11274.
13 D. Montarnal, M. Capelot, F. Tournilhac and L. Leibler, *Science*, 2011, **334**, 965–968.
14 M. A. Lucherelli, A. Duval and L. Avérous, *Prog. Polym. Sci.*, 2022, **127**, 101515.
15 A. Adjaoud, A. Trejo-Machin, L. Puchot and P. Verge, *Polym. Chem.*, 2021, **12**, 3276–3289.
16 B. R. Elling and W. R. Dichtel, *ACS Cent. Sci.*, 2020, **6**, 1488–1496.
17 Z. Wei, J. H. Yang, Z. Q. Liu, F. Xu, J. X. Zhou, M. Zrínyi, Y. Osada and Y. M. Chen, *Adv. Funct. Mater.*, 2015, **25**, 1352–1359.
18 G. Banerjee and P. Chattopadhyay, *J. Sci. Food Agric.*, 2019, **99**, 499–506.
19 R. Li, P. Zhang, T. Liu, B. Muhunthan, J. Xin and J. Zhang, *ACS Sustainable Chem. Eng.*, 2018, **6**, 4016–4025.
20 H. Peng, H. Xiong, J. Li, M. Xie, Y. Liu, C. Bai and L. Chen, *Food Chem.*, 2010, **121**, 23–28.
21 Z. Guo, B. Liu, L. Zhou, L. Wang, K. Majeed, B. Zhang, F. Zhou and Q. Zhang, *Polymer*, 2020, **197**, 122483.
22 S. Wang, S. Ma, Q. Li, W. Yuan, B. Wang and J. Zhu, *Macromolecules*, 2018, **51**, 8001–8012.
23 S. Dhers, G. Vantomme and L. Avérous, *Green Chem.*, 2019, **21**, 1596–1601.

24 M. Hakkarainen, Y. Xu and K. Odelius, *ACS Sustainable Chem. Eng.*, 2020, **8**, 17272–17279.
25 S. Wang, S. Ma, Q. Li, X. Xu, B. Wang, K. Huang, Y. Liu and J. Zhu, *Macromolecules*, 2015, **48**, 2407–2416.
26 Q. Yu, X. Peng, Y. Wang, H. Geng, A. Xu, X. Zhang, W. Xu and D. Ye, *Eur. Polym. J.*, 2019, **117**, 55–63.
27 J. T. Miao, L. Yuan, Q. Guan, G. Liang and A. Gu, *ACS Sustainable Chem. Eng.*, 2017, **5**, 7003–7011.
28 Y. Tian, Q. Wang, Y. Hu, H. Sun, Z. Cui, L. Kou, J. Cheng and J. Zhang, *Polymer*, 2019, **178**, 121592.
29 Y. Liu, J. Zhao, Y. Peng, J. Luo, L. Cao and X. Liu, *Ind. Eng. Chem. Res.*, 2020, **59**, 1914–1924.
30 J. Wan, B. Gan, C. Li, J. Molina-Aldareguia, E. N. Kalali, X. Wang and D. Y. Wang, *Chem. Eng. J.*, 2016, **284**, 1080–1093.
31 J. Wan, B. Gan, C. Li, J. Molina-Aldareguia, Z. Li, X. Wang and D. Y. Wang, *J. Mater. Chem. A*, 2015, **3**, 21907–21921.
32 S. H. Park, A. Alammar, Z. Fulop, B. A. Pulido, S. P. Nunes and G. Szekely, *Green Chem.*, 2021, **23**, 1175–1184.
33 Y. Tian, Q. Wang, J. Cheng and J. Zhang, *Green Chem.*, 2020, **22**, 921–932.
34 L. Jiang, Y. Tian, J. Cheng and J. Zhang, *Polym. Chem.*, 2021, **12**, 6527–6537.
35 H. Zheng, Q. Liu, X. Lei, Y. Chen, B. Zhang and Q. Zhang, *J. Polym. Sci., Part A: Polym. Chem.*, 2018, **56**, 2531–2538.
36 K. Hong, Q. Sun, X. Zhang, L. Fan, T. Wu and J. Du, *ACS Sustainable Chem. Eng.*, 2022, **10**, 1036–1046.